International Journal of Heat and Mass Transfer 52 (2009) 142–150

Contents lists available at ScienceDirect

International Journal of Heat and Mass Transfer

journal homepage: www.elsevier.com/locate/ijhmt

Experimental investigation of convective heat transfer coefficient during downward laminar flow condensation of R134a in a vertical smooth tube

A.S. Dalkilic [a,*], S. Yildiz [a], S. Wongwises [b,*]

[a] Heat and Thermodynamics Division, Department of Mechanical Engineering, Yildiz Technical University, Yildiz, Istanbul 34349, Turkey
[b] Fluid Mechanics, Thermal Engineering and Multiphase Flow Research Laboratory (FUTURE), Department of Mechanical Engineering, King Mongkut's University of Technology Thonburi, Bangmod, Bangkok 10140, Thailand

ARTICLE INFO

Article history:
Received 12 February 2008
Received in revised form 31 May 2008
Available online 15 August 2008

Keywords:
Condensation
Heat transfer coefficient
Downward flow
Laminar flow

ABSTRACT

This paper presents an experimental investigation of laminar film condensation of R134a in a vertical smooth tube having an inner diameter of 7–8.1 mm and a length of 500 mm. Condensation experiments were performed at mass fluxes of 29 and 263 kg m^{-2} s^{-1}. The pressures were between 0.77 and 0.1 MPa. The heat transfer coefficient, film thickness and condensation rate during downward condensing film were determined. The results show that an interfacial shear effect is significant for the laminar condensation heat transfer of R134a under the given conditions. A new correlation for the condensation heat transfer coefficient is proposed for practical applications.

1. Introduction

Annular flow along a tube length, including convective condensation, occurs in many real applications. It is one of the most important flow regimes and is characterised by a phase interface separating a thin liquid film from the gas flow in the core region. Because of its practical importance and the relative ease with which analytical treatment may be applied, this flow regime has received the most attention both analytically and experimentally.

Nusselt [1] proposed the first theoretical solution for predicting heat transfer coefficients. He assumed a linear temperature profile through a laminar film flowing downwards without entrainment on a vertical plate. Waves and an interfacial shear effect between the phases were not considered. Under these conditions, it is possible for the Nusselt-type analysis to be used for convective condensation in round tubes.

Rohsenov [2] and Dukler [3] developed a model to predict momentum transfer for turbulent film flow. In addition to this, Levich [4] and Blangetti et al. [5] used a model to estimate the local heat transfer coefficients of the film. An empirical relationship between the Fanning friction factor and vapour Reynolds number for an annular flow regime was proposed by Bergelin et al. [6]. They studied the pressure drop of air–water and several organic vapours for the downward turbulent flow through a vertical 25.4 mm i.d. tube. Their diagram was used by several researchers such as Blangetti et al. [5] and Maheshwari et al. [7] for various refrigerants. The diagram takes account of the effect of mass transfer by including a correction factor developed by Bird et al. [8], considering the effect of suction in condensation. Krebs and Schlunder [9] investigated mass transfer coefficients in the turbulent gas and film flow of a vertical condenser tube in the presence of non-condensing gases. Kuhn et al. [10,11] investigated local condensation heat transfer in the presence of non-condensable gases inside a vertical tube connecting a passive containment cooling system (PCCS). They studied the degradation factor method, diffusion layer theory and mass transfer conductance model. Recently, Maheshwari et al. [7] followed the same path and adopted the model, using the analogy between heat and mass transfer, to the PCCS in nuclear reactors. They considered non-condensable gas with a wide range of Reynolds numbers in their investigation. The film waviness effect on the gas/vapour boundary layer, the suction effect due to condensation, and the developing flow and property variation of the gas were also considered in their study. Local film heat transfer coefficients were multiplied by a factor of 1.28 for the wave effect between the phases in the high mass flux region. In addition to this, Oh and Revankar [12] studied the vertical passive condenser (PCCS) for complete condensation in nuclear reactors. They used a similar analysis model as [2–11]. Their model includes a modified Nusselt theory with a Mc Adams correction factor of 1.2 [13], the Blangetti model [5] and interfacial shear from the Couette flow analysis [14] for small film Reynolds numbers and small interfacial shear conditions.

* Corresponding authors. Tel.: +902122597070; fax: +902122616659 (A.S. Dalkilic); tel.: +6624709115; fax: +6624709111 (S. Wongwises).
E-mail addresses: dalkilic@yildiz.edu.tr (A.S. Dalkilic), Somchai.won@kmutt.ac.th (S. Wongwises).

0017-9310/$ - see front matter © 2008 Published by Elsevier Ltd.
doi:10.1016/j.ijheatmasstransfer.2008.05.035

Nomenclature

A_i	tube inside surface area, m^2
C_p	specific heat capacity at constant pressure, J kg^{-1} K^{-1}
D	inside diameter of tube, m
G	mass flux, kg m^{-2} s^{-1}
g	gravitational acceleration, m s^{-2}
h	heat transfer coefficient, W m^{-2} K^{-1}
h_{fg}	latent heat of condensation, J kg^{-1}
k	thermal conductivity, W m^{-1} K^{-1}
L	tube length, m
$\dot{m}$	mass flow rate, kg s^{-1}
Nu	Nusselt number
P	pressure, MPa
Pr	Prandtl number
Re	Reynolds number
$\dot{q}$	heat transfer rate, W
q''	heat flux, W m^{-2}
Q	volumetric flow rate, m^3 s^{-1}
T	temperature, °C
u	axial velocity, m s^{-1}
U	overall heat transfer coefficient, W m^{-2} K^{-1}
x	vapour quality
X	Lockhart Martinelli parameter
y	wall coordinate
z	axial coordinate
ΔT_{sat}	$T_{sat} - T_{wi}$, °C
α	void fraction

Greek symbols

δ	film thickness, m
μ	dynamic viscosity, kg m^{-1} s^{-1}
ν	kinematic viscosity, m^2 s^{-1}
ρ	density, kg m^{-3}
ρ_g^*	fictitious vapour density defined by Carey [15], kg m^{-3}
τ	shear stress, N m^{-2}

Subscripts

avg	average
corr	correlation
eq	equivalent
exp	experimental
evap	evaporator
F	frictional term
G	gravitational term
g	gas/vapour
i	inlet
l	liquid
M	momentum term
o	outlet
r	refrigerant
sat	saturation
t	test section
T	total
w	water
wi	inner wall

Carey's method [15] for the solution of convective condensation in round tubes during an annular flow regime was investigated in this paper. He applied Nusselt's theory [1] with interfacial shear stress, added new simplified equations, and offered an iterative technique for the computation of interfacial shear and the determination of the local heat transfer coefficients at the end. He assumed constant thermophysical properties of the refrigerant for condensation and noted that the pressure drop along the test tube was small. Besides this, he stated that his analysis was not appropriate for full or partial turbulent film flow.

In-tube condensation of refrigerants has been studied by a number of researchers. However, it should be noted that most of the ranges of reported mass flux in their studies are low. Relatively little information is currently available on the heat transfer characteristics of two-phase cocurrent annular flow in a vertical pipe for the high mass flux region. In the present study, the main aim was to extend the existing heat transfer database to the high mass flux region of HFC-134a during condensation in a small diameter vertical smooth tube. Moreover, the alteration of local heat transfer coefficients, film thickness, and the condensation rates along the test tube were investigated, and several existing correlations were compared to show the significance of interfacial shear stress. In addition, a new correlation for the condensation heat transfer coefficient is proposed for practical applications.

2. Experimental setup

2.1. Test facility

A schematic diagram of the test apparatus is shown in Fig. 1. The refrigerant loop consists of an evaporator, test section and condenser loop. The refrigerant is circulated by a gear pump controlled by an inverter. The refrigerant flows in series through the bypass line, a coriolis type refrigerant flow meter which has a sensitivity of 0.1%, an evaporator, a separator, and a sight glass tube and enters the test section. The evaporator controls the inlet quality before entering the test section, and consists of a plate heat exchanger designed to supply heat to adjust the inlet quality for the vapourisation of the refrigerant. The circulated water flow rate of the evaporator is measured by a turbine-type flow meter which has a sensitivity of 2%. After exiting the test section, the vapour phase of R134a, which comes from the liquid–gas separator, continues to the condenser. The flow rate of liquid R134a from the liquid–gas separator is measured in a vessel to check the conditions of the apparatus. A plate heat exchanger is used as a condenser. The liquid phase of R134a, from the condenser and separator, is collected in a reserve tank which has a water coil to balance the pressure of liquid R134a. There is another sight glass to check the saturated liquid R134a before the refrigerant pump. The pressures are measured by pressure transducers which have sensitivities of 0.5%.

The test section is a vertical counter-flow tube-in-tube heat exchanger with refrigerant flowing in the inner tube and cooling water flowing in the annulus. The inner and outer tubes are made from smooth vertical copper having an inner diameter of 7–8.1 and 16–19 mm, respectively. The length of the heat exchanger is 0.5 m. A thermostat is used to control the inlet temperature of the water. The flow rate of cooling water is measured using a turbine-type flow meter which has a sensitivity of 1%. Pressure drop is measured by a differential pressure transducer, which has a sensitivity of 0.05%, installed between the inlet and outlet of the test section. The temperatures of the inlet and outlet of the test section are measured by pt100 sensors and T-type thermocouples. A band-type heater is wrapped around the copper tube line from the exit of the evaporator to the inlet of the test tube to control the system pressure of the refrigerant flow.

A PLC device was used to record and collect data from all flow meters, pressure transducers and differential pressure transmitters. The computer program collected 10 types of data and recorded the average values each second using an MS Excel program spreadsheet.

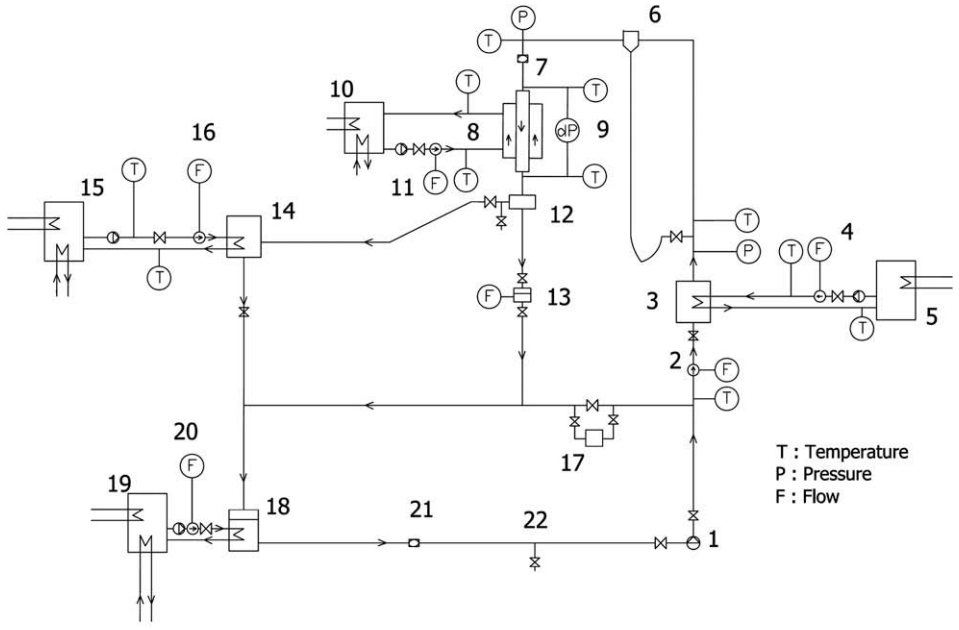

1 - Refrigerant Pump 2 - Coriolis Flow Meter 3- Evaporator 4- Turbine Flow Meter
5 - Thermostat System 6 - Liquid/Gas Seperator 7 - Sight Glass 8 - Test Section
9 - Differancial Pressure Transmitter 10 - Thermostat System 11 - Turbine Flow Meter
12 - Liquid/Gas Seperator 13- Scaled Vessel 14 - Condenser 15 - Thermostat System
16 - Rotameter 17- Filter/Dryer 18 - R134a Reserve Tank 19 - Thermostat System
20 - Rotameter 21- Sight Glass 22 - R134a Charging Point

Fig. 1. Schematic diagram of experimental apparatus [18].

Special attention was given to experimental accuracy. T-type thermocouples were used to measure refrigerant temperature and the tube wall temperatures in the test section. Fig. 2 shows a total of ten thermocouples located at the side, at five points along the test tube. All the temperature measuring devices were carefully calibrated in a controlled-temperature bath using standard precision mercury glass thermometers. The uncertainty of the temperature measurements was 0.1 K. All static pressure taps were mounted on the tube wall. The refrigerant flow meter was specially calibrated in the range of 0–10 l h^{-1} for HFC-134a by the manufacturer. The

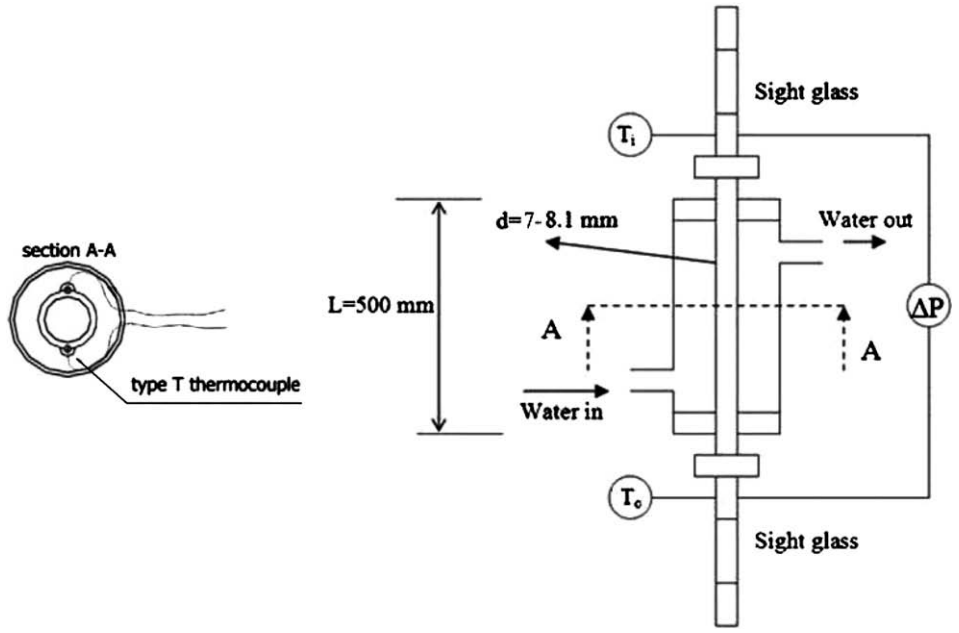

Fig. 2. Schematic diagram of test section.

differential pressure transducer and pressure gauges were calibrated against a primary standard, the dead weight tester.

2.2. Data reduction

The following equations were used to prepare the system for experiments which had a saturated vapour of R134a at the inlet of the test section during steady-state regime conditions. Separate energy balances are given for the evaporator and test section. The thermodynamics and transport properties of the refrigerant were evaluated with the REFPROP computer program, version 6.01 [19]. The data reduction of the measured results is summarised below:

2.2.1. Evaporator

The total heat transfer rate from hot water to liquid R134a in the evaporator is the sum of the latent and sensible heat transfer rates:

$$\dot{q}_{\text{evap}} = \dot{q}_{\text{r,sensible}} + \dot{q}_{\text{r,latent}} = \dot{m}_{\text{w}} C_{\text{p,w}} (T_{\text{w,i}} - T_{\text{w,o}}) \tag{2.1}$$

$$\dot{q}_{\text{sensible}} = \dot{m}_{\text{r,T}} . C_{\text{p,R134a}} . (T_{\text{evap,o}} - T_{\text{evap,i}}) \tag{2.2}$$

$$\dot{q}_{\text{latent}} = \dot{m}_{\text{r,T}} . h_{\text{fg}} . (x_{\text{evap,o}} - x_{\text{evap,i}}) \tag{2.3}$$

2.2.2. Test section

The outlet quality of R134a from the evaporator is equal to the quality of R134a at the test section inlet. From the energy balance in the test section, the inlet quality of R134a is given below as ($x_{\text{evap,i}} = 0$, $x_{\text{evap,o}} = x_{\text{t,i}} = 1$):

$$x_{\text{o,evap}} = \frac{1}{h_{\text{fg}}} \left[\frac{\dot{q}_{\text{evap}}}{\dot{m}_{\text{r,T}}} - c_{\text{p,r}} (T_{\text{r,sat}} - T_{\text{r,i}}) \right] \tag{2.4}$$

The heat transfer rate from saturated R134a to the cold water in the annulus is

$$\dot{q}_{\text{t}} = \dot{m}_{\text{w}} . C_{\text{p,w}} . (T_{\text{w,o}} - T_{\text{w,i}}) \tag{2.5}$$

The vapour quality alteration in the test section is

$$\Delta x = \frac{\dot{q}_t}{\dot{m}_{\text{r,T}} h_{\text{fg}}} \tag{2.6}$$

The experimental condensation heat transfer coefficient in the test tube can be expressed as:

$$h_{\text{exp}} = \dot{q}_{\text{t}} / (A_{\text{i}} . (T_{\text{r,sat}} - T_{\text{wi}})) \tag{2.7}$$

2.2.3. Uncertainties

The procedure of Kline and McClintock [17] was used for the calculation of all uncertainties.

The maximum uncertainties of experimental parameters are shown in Table 1. The largest uncertainties occurred in the low mass flux region. The uncertainties for the Nusselt number and condensation heat transfer coefficient in the test tube varied from ±7.64% to ±10.71%.

Table 1
Uncertainty of experimental parameters

Parameters	Uncertainty
$T_{\text{r,sat}}$ (°C)	0.19
$x_{\text{t,i}}$ (%)	±6.96–8.24%
ΔT_{sat} (K)	±0.191
$(T_{\text{w,o}} - T_{\text{w,i}})_{\text{t}}$ (K)	±0.045
$(T_{\text{w,i}} - T_{\text{w,o}})_{\text{evap}}$ (K)	±0.13
$\dot{m}_{\text{r}}$ (g s^{-1})	±0.023
$\dot{m}_{\text{w,t}}$ (g s^{-1})	±0.35
$\dot{m}_{\text{w,evap}}$ (g s^{-1})	±0.38
$\dot{q}_{\text{t}}$ (kW m^{-2})	±6.55–8.93%
$\dot{q}_{\text{evap}}$ (kW m^{-2})	±12–14.81%
Nu	±7.64–10.71%
h_{r} (W m^{-2} K^{-1})	±7.64–10.71%

3. The laminar annular film condensation model

The steady-state physical model of downward film condensation of R134a in a vertical tube is shown in Fig. 3. The following assumptions were made: laminar film flow; saturated state for the vapour of R134a; condensed film of R134a along the tube surface; constant physical properties corresponding to inlet pressure and temperature conditions; no entrainment. Under these assumptions, the internal convective condensation in a round tube can be investigated using a Nusselt-type analysis. The interfacial shear effect at the interface is considered because the vapour velocity is much greater than the film velocity.

The force balance for the differential element in the control volume is shown below (it should be noted that the inertia and downstream diffusion contributions were ignored).

$$\rho_{\text{l}} g \mathrm{d}x\mathrm{d}y\mathrm{d}z + \tau_\delta(y + \mathrm{d}y)\mathrm{d}x\mathrm{d}z + P(z)\mathrm{d}x\mathrm{d}y = \tau_\delta(y)\mathrm{d}x\mathrm{d}z + P(z + \mathrm{d}z)\mathrm{d}x\mathrm{d}y \tag{3.1}$$

The two-phase pressure gradient is the sum of three contributions: the hydrostatic pressure gradient, the frictional pressure gradient and the momentum pressure gradient, and can be shown as:

$$\left(\frac{\mathrm{d}P}{\mathrm{d}z}\right)_{\text{T}} = \left(\frac{\mathrm{d}P}{\mathrm{d}z}\right)_{\text{G}} + \left(\frac{\mathrm{d}P}{\mathrm{d}z}\right)_{\text{F}} + \left(\frac{\mathrm{d}P}{\mathrm{d}z}\right)_{\text{M}} \tag{3.2}$$

where the hydrostatic pressure gradient can be expressed as

$$\left(\frac{\mathrm{d}P}{\mathrm{d}z}\right)_{\text{G}} = \rho_{\text{g}} g \tag{3.3}$$

The frictional pressure gradient in the vapour, which is caused by the interfacial shear stress [15], is

$$\left(\frac{\mathrm{d}P}{\mathrm{d}z}\right)_{\text{F}} = -\frac{4\tau_\delta}{(D - 2\delta)} \tag{3.4}$$

The momentum pressure gradient can be written according to the results of the one-dimensional two-phase separated-flow analysis:

$$\left(\frac{\mathrm{d}P}{\mathrm{d}z}\right)_{\text{M}} = -G^2 \frac{\mathrm{d}}{\mathrm{d}z} \left[\frac{x^2}{\rho_{\text{g}} \alpha} + \frac{(1 - x)^2}{\rho_{\text{l}} (1 - \alpha)} \right] \tag{3.5}$$

Eq. (3.5) can be simplified to Eq. (3.6) under the following assumptions: vapour density of R134a is very low when compared with its liquid density; the variation in the void fraction along the test tube is small compared to the variation in vapour quality [15]:

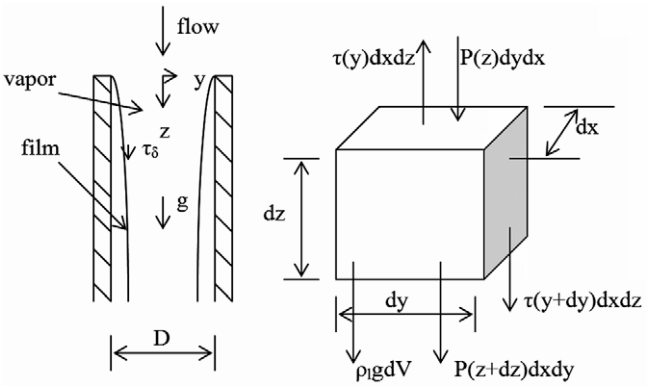

Fig. 3. System model for analysis of downward condensation.

$$\left(\frac{dP}{dz}\right)_M = -\frac{2xDG^2}{\rho_g(D-2\delta)}\frac{dx}{dz} \tag{3.6}$$

Carey [15] adapted this by means of the usual idealisation on pressure gradient which has an equal value in the vapour phase and in the liquid film. He defined a fictitious vapour density to facilitate analysis of the momentum transport in the liquid film, as shown below [15]:

$$\rho_g^* g = \rho_g g - \frac{4\tau_\delta}{D-2\delta} - \frac{2xDG^2}{\rho_g(D-2\delta)}\left(\frac{dx}{dz}\right) \tag{3.7}$$

Using interfacial shear stress, the velocity gradient is shown as follows:

$$\frac{du}{dy} = \frac{(\delta-y)(\rho_l-\rho_g^*)g}{\mu_l} + \frac{\tau_\delta}{\mu_l} \tag{3.8}$$

Eq. (3.8) can be integrated using $u = 0$ at $y = 0$ to obtain:

$$u = \frac{(\rho_l-\rho_g^*)g}{\mu_l}\left(y\delta - \frac{y^2}{2}\right) + \frac{\tau_\delta y}{\mu_l} \tag{3.9}$$

The liquid flow rate can be calculated from the velocity profile:

$$\dot{m} = \pi D\delta u_{avg}\rho_l = \left[\frac{(\rho_l-\rho_g^*)g\delta^2}{3\mu_l} + \frac{\tau_\delta\delta}{2\mu_l}\right]\pi D\delta\rho_l \tag{3.10}$$

From the overall mass and energy balance in the case of a falling film without subcooling [15]:

$$k_l\left(\frac{T_{r,sat}-T_{w,i}}{\delta}\right)\pi D dz = h_{fg}\, d\dot{m} \tag{3.11}$$

The quality gradient can be obtained from the energy balance as [15]:

$$\dot{q} = h_l\pi D\Delta z\Delta T_{sat} = \dot{m}_{cond}h_{fg} \tag{3.12}$$

$$\frac{dx}{dz} = \frac{4q''}{DGh_{fg}} = \frac{4h_l(T_{r,sat}-T_{w,i})}{DGh_{fg}} \tag{3.13}$$

Eq. (3.11) can be rearranged using Eq. (3.13): ($\delta = 0$, $x = 0$)

$$\delta^4 + \frac{4}{3}\frac{\tau_\delta\delta^3}{(\rho_l-\rho_g^*)g} = \frac{4k_l\mu_l(T_{r,sat}-T_{w,i})z}{\rho_l(\rho_l-\rho_g^*)gh_{fg}} \tag{3.14}$$

If we omit the interfacial shear stress effect (the Nusselt analysis with no interfacial shear), the film thickness can be evaluated as:

$$\delta(z) = \left[\frac{4\mu_l k_l z(T_{r,sat}-T_{w,i})}{gh_{fg}\rho_l(\rho_l-\rho_g)}\right]^{1/4} \tag{3.15}$$

The correction factor for the latent heat of vapourisation per unit mass can be applied to Eq. (3.14) as follows:

$$h'_{fg} = h_{fg}\left[1 + \left(\frac{3}{8}\right)\frac{c_{pl}(T_{r,sat}-T_{w,i})}{h_{fg}}\right] \tag{3.16}$$

A linear temperature distribution in the film region is assumed for a laminar film and the film heat transfer coefficient can be expressed as:

$$h_l(z) = \frac{k_l}{\delta(z)} \tag{3.17}$$

As an approximation, the vapour flow in the tube can be treated as a single phase flow. Because the film is thin, the mean velocity of vapour is much larger than the liquid velocity at the interface due to the high viscosity of the liquid phase compared to the vapour phase. Moreover, vapour velocity is assumed to be zero between the phases. The interfacial shear can be computed using the conventional single phase correlation by using these assumptions [15]:

$$\tau_\delta = f_g\left(\frac{\rho_g u_g^2}{2}\right) = f_g\left(\frac{G^2x^2}{2\rho_g(1-4\delta/D)}\right) \tag{3.18}$$

The friction factor for round tubes can be evaluated as follows [15]:

$$f_g = 0.079\left[\frac{Gx(D-\delta)}{\mu_g(1-4\delta/D)}\right]^{-0.25} \tag{3.19}$$

The McAdams correction factor [13] can be used to consider the effects of the waviness and rippling in the film on the increase in heat transfer. It is recommended for downward laminar film condensation, and modifies the Nusselt equation as follows:

$$h_{wave} = 1.2\frac{k_l}{\delta(z)} \tag{3.20}$$

The film heat transfer coefficient and interfacial shear can be determined using an iterative technique for specified mass flux, tube wall inlet temperature, condensation pressure and thermophysical properties. After estimating a value for film thickness, Eqs. (3.13) and (3.17) should be used to evaluate the quality gradient. By means of Eqs. (3.18) and (3.19), interfacial shear can be calculated. The fictitious vapour density is obtained from Eq. (3.7). The estimated film thickness values, calculated fictitious vapour density and interfacial shear values are substituted into Eq. (3.14). These values are updated and the film thickness value repeatedly estimated until convergence. If the level of accuracy is acceptable, the values of estimated film thickness and calculated film heat transfer coefficient are correct. This procedure can also be seen in Fig. 4.

Nusselt's theory for condensation on vertical flat surfaces can also be used for condensation inside and outside the tubes if the tubes are large in diameter, compared with the film thickness. According to Nusselt [1], the convective heat transfer coefficient is shown as follows ($0 < Re_l < 30$):

$$h_{Nusselt} = 0.943\left[\frac{\rho_l(\rho_l-\rho_g)gh_{fg}k_l^3}{\mu_l L(T_{r,sat}-T_{w,i})}\right]^{1/4} \tag{3.21}$$

4. Results and discussion

Experiments were carried out with R134a for mass fluxes of 29–263 kg m^{-2} s^{-1} and pressures between 0.77 and 0.1 MPa in a smooth tube. All local heat transfer coefficients were calculated using the modified Nusselt theory which included the interfacial shear effect. The effect of the temperature difference between the saturated temperature of the vapour and the inlet wall temperature of the tube (ΔT_{sat}) and the condensation pressure on the local heat transfer coefficients, film thickness and condensation rates along the tube length are shown in Figs. 5–10.

Figs. 5–7 show that the condensation heat transfer coefficient decreases along the tube length because the film thickness and hence total condensation rate increase from the top to the bottom of the test tube as the driving force of condensation. The local condensation rate along the tube length is high at the tube entrance due to high vapour velocity and high interfacial shear. It decreases along the tube length with decreasing vapour velocity due to an increase in condensation rate. Oh and Revankar [12] obtained similar results.

Figs. 8–10 show the effect of pressure, in other words, the effect of the saturation temperature on the local heat transfer coefficients, film thickness and condensation rate along the tube length for a smooth tube. Low condensation pressures, in other words, high temperature differences and alteration of physical properties at low pressure, cause higher local heat transfer coefficients than

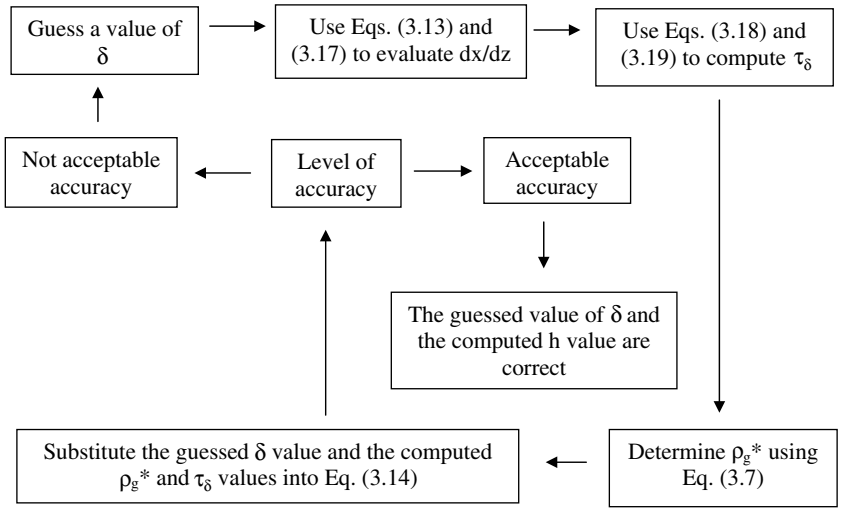

Fig. 4. Flow chart of iteration process [15].

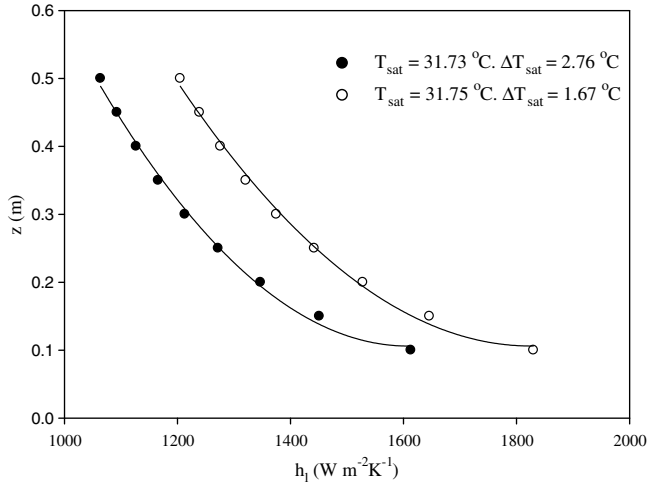

Fig. 5. Comparison of local heat transfer coefficients at different ΔT_{sat} for the mass flux of 29 kg m^{-2} s^{-1} and condensation pressure of 0.8 MPa.

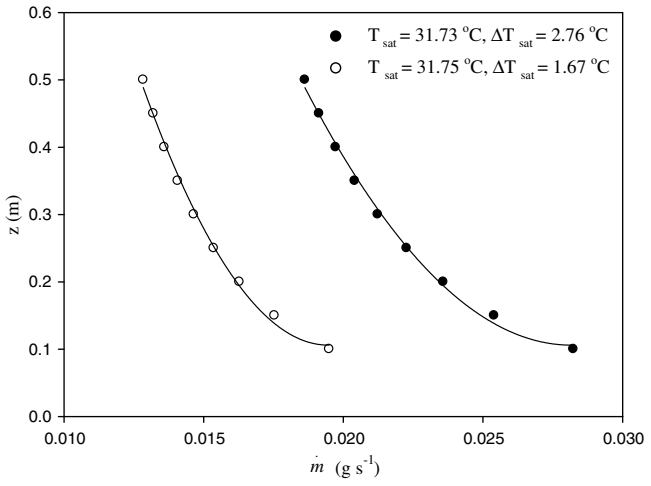

Fig. 7. Comparison of local condensation rates at different ΔT_{sat} for the mass flux of 29 kg m^{-2} s^{-1} and condensation pressure of 0.8 MPa.

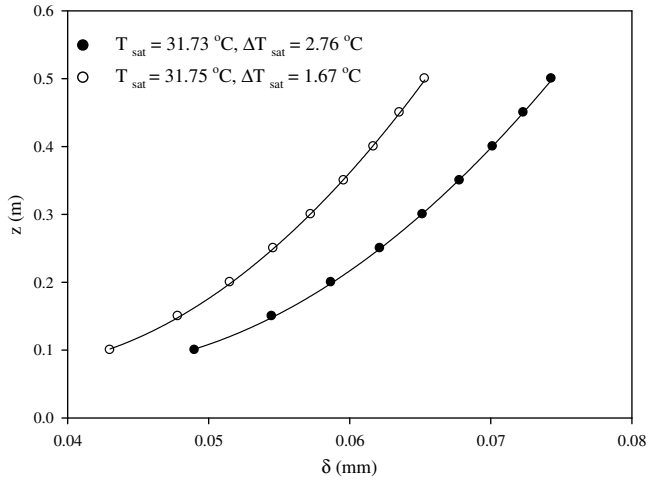

Fig. 6. Comparison of local film thickness at different ΔT_{sat} for the mass flux of 29 kg m^{-2} s^{-1} and condensation pressure of 0.8 MPa.

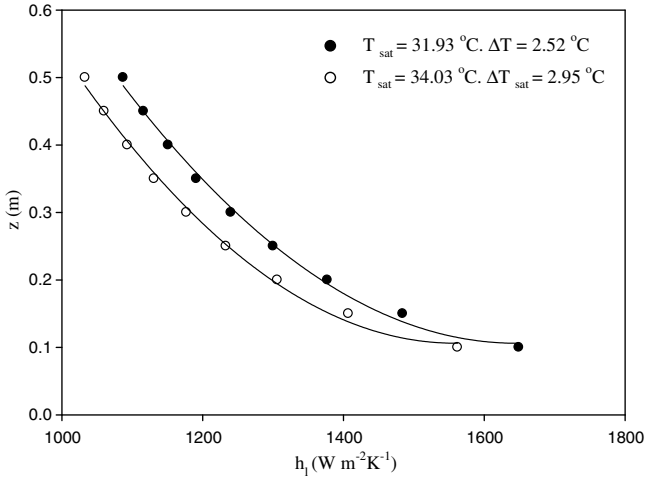

Fig. 8. Comparison of local heat transfer coefficients at different ΔT_{sat} and different condensation pressures (0.8–0.85 MPa) for the mass flux of 29 kg m^{-2} s^{-1}.

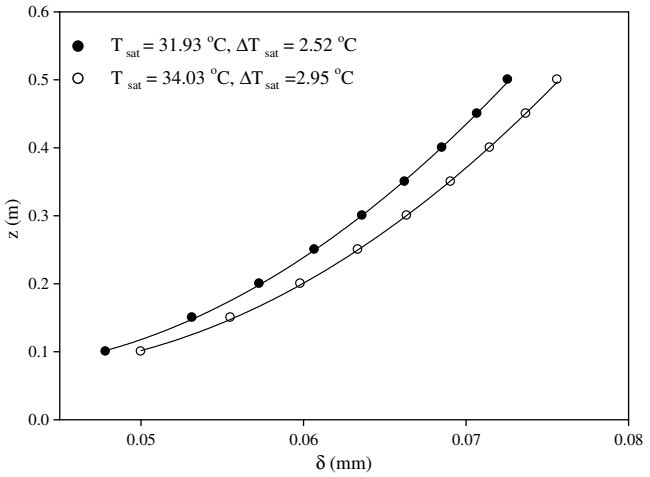

Fig. 9. Comparison of local film thickness at different ΔT_{sat} and different condensation pressures (0.8–0.85 MPa) for the mass flux of 29 kg m^{-2} s^{-1}.

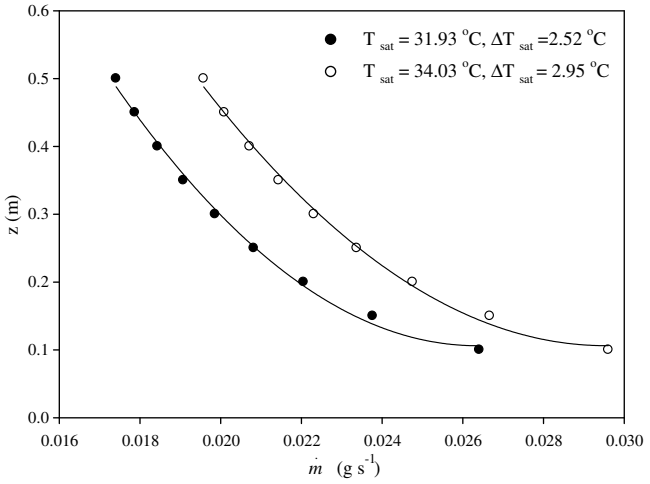

Fig. 10. Comparison of local condensation rates at different ΔT_{sat} and different condensation pressures (0.8–0.85 MPa) for the mass flux of 29 kg m^{-2} s^{-1}.

high condensation pressure. These results and the general trend are consistent with the Nusselt [1] theory in which the average and local heat transfer coefficients are proportional to $\Delta T_{sat}^{-0.25}$ and $z^{-0.25}$.

4.1. Comparison with the existing models

The modified Nusselt theory [15], the McAdams correlation [13] and the classical Nusselt theory [1] were used to determine the film heat transfer coefficient for the laminar flow at low mass flux.

According to Fig. 11, the modified Nusselt theory in Eq. (3.14), which included the interfacial shear stress effect, is the most suitable model for the experimental data from the smooth tube. Moreover, Fig. 11 shows that studies do not need the McAdams correction factor in Eq. (3.20) for the wave effect at the vapour–liquid interface due to low mass flux. In addition, the classical Nusselt theory in Eq. (3.21) predicts data over 30% deviation and overestimates the heat transfer coefficients.

The modified Nusselt theory [15], the McAdams correlation [13], the classical Nusselt theory [1], the Dobson and Chato model [20], the Fujii correlation [21] and the Cavallini et al. correlation [22] were used to investigate the film heat transfer coefficients during laminar flow at high mass flux.

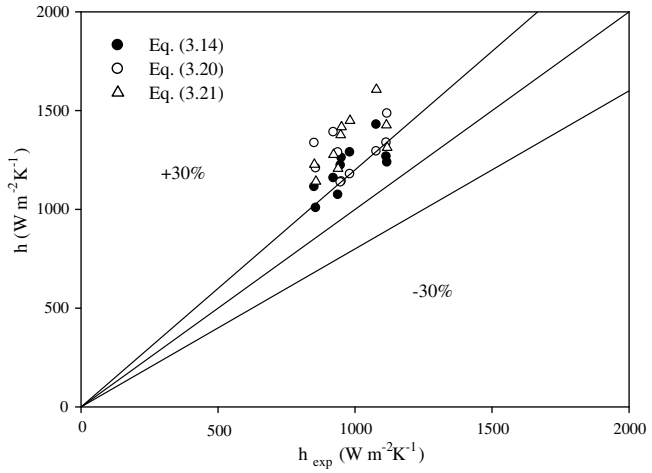

Fig. 11. Comparisons between the experimental and calculated condensation heat transfer coefficients for the smooth tube under the experimental conditions: G = 29 kg m^{-2} s^{-1}, P = 0.8–0.85 MPa, T_{sat} = 31.73–34.03 °C, ΔT_{sat} = 1.67–2.95 °C, x_{avg} = 0.93–0.99.

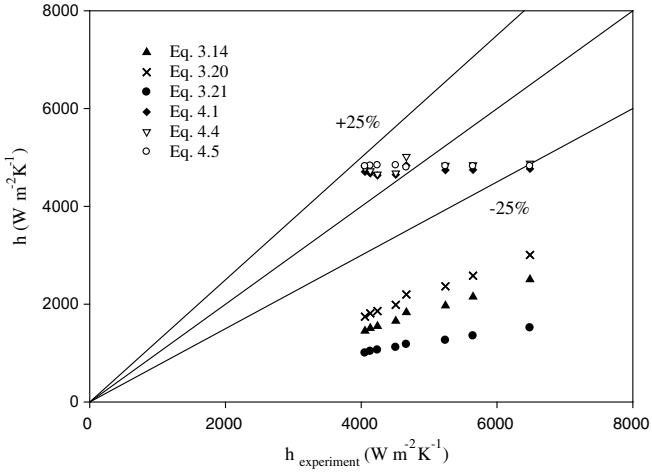

Fig. 12. Comparisons between the experimental and calculated condensation heat transfer coefficients for the smooth tube under the experimental conditions: G = 263 kg m^{-2} s^{-1}, P = 0.1 MPa, T_{sat} = 40 °C, ΔT_{sat} = 1.56–8.58 °C, x_{avg} = 0.91–0.97.

According to Fig. 12, the modified Nusselt theory's [15] deviation is between 60.7% and 64.1%, the McAdams correlation's [13] deviation is between 52.8% and 56.9%, and the classical Nusselt theory's [1] deviation is between 74.7% and 76.6%. This shows that they are not suitable for laminar flow at high mass flux. These correlations are usually applied to stationary vapour flow. They are not valid when the vapour velocity is much greater than the film velocity along the test tube. High vapour velocity can also cause dragging on the downward motion of the condensate. The Nusselt-type analysis does not take account of high vapour friction or momentum drag. In addition, it is useful to know that for the solution of laminar flow at high mass flux, the deviations of the Dobson and Chato model [20], the Fujii correlation [21] and Cavallini et al.'s correlation [22] are within the range of ±25%.

Dobson and Chato's model, Fujii's correlation and Cavallini et al.'s correlation are well-known correlations for the annular flow regime. Based on Hewitt and Robertson's [23] flow pattern map, the data shown in Figs. 11 and 12 were collected in an annular flow regime and also checked by sight glass at the inlet and outlet of the test section. In the present study, these correlations are used to

show the similarity of annular flow correlations which are independent of tube orientation (horizontal or vertical). Chen et al. [24] also mentioned this similarity in their article.

4.1.1. Dobson and Chato model

Dobson and Chato [20] developed a correlation (Eq. (4.1)) using a two-phase multiplier for the annular flow regime. Their correlations are commonly used for zeotropic refrigerants and are recommended for $G > 500\ \mathrm{kg\ m^{-2}\ s^{-1}}$ for all qualities in horizontal tubes.

$$Nu_l = 0.023 Re_l^{0.8} Pr_l^{0.4}\left[1 + \frac{2.22}{X^{0.89}}\right] \tag{4.1}$$

where

$$Re_l = \frac{GD(1-x)}{\mu_l} \tag{4.2}$$

$$X = \left(\frac{1-x}{x}\right)^{0.9}\left(\frac{\rho_g}{\rho_l}\right)^{0.5}\left(\frac{\mu_l}{\mu_g}\right)^{0.1} \tag{4.3}$$

4.1.2. Fujii correlation

Fujii [21] developed the following correlation for smooth tubes used for shear-controlled regimes:

$$Nu_l = 0.0125\left(Re_l\sqrt{\rho_l/\rho_g}\right)^{0.9}\left(\frac{x}{1-x}\right)^{0.1x+0.8} Pr_l^{0.63} \tag{4.4}$$

4.1.3. Cavallini et al. correlation

Cavallini et al. [22] developed a semi-empirical correlation for the condensation of various organic refrigerants in both vertical and horizontal orientations. It is as follows:

$$Nu_l = 0.05 Re_{eq}^{0.8} Pr^{0.33} \tag{4.5}$$

where

$$Re_{eq} = Re_g(\mu_g/\mu_l)(\rho_l/\rho_g)^{0.5} Re_l \tag{4.6}$$

and Re_l is defined in Eq. (4.2).

4.2. Comparison of the average convective heat transfer coefficients for the smooth tube

The effect of the condensation pressure on the heat transfer coefficients is shown in Fig. 13. The average experimental condensation heat transfer coefficients obtained from Eq. (2.7) decrease with increasing system pressure as explained previously.

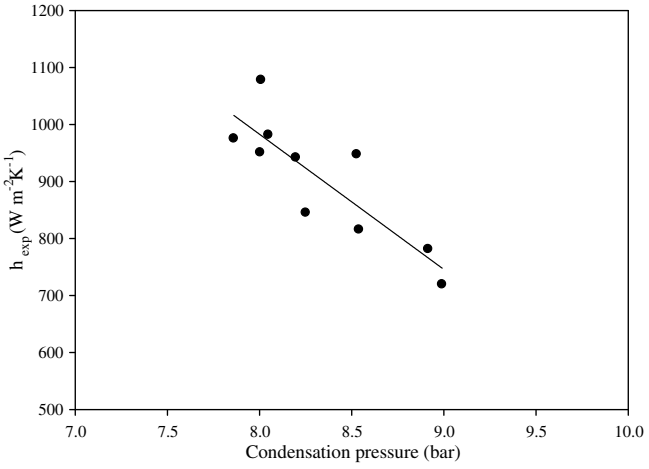

Fig. 13. Comparison of average experimental convective heat transfer coefficients for the mass flux of 29 at pressures of 0.77–0.90 MPa.

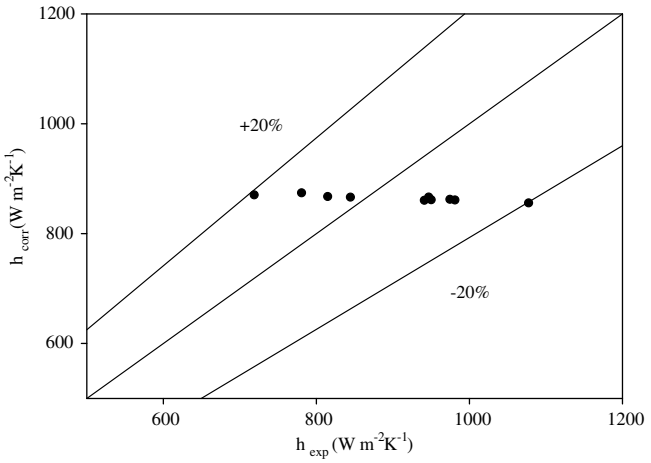

Fig. 14. Comparison of the experimental convective heat transfer coefficient with the present heat transfer correlation Eq. (4.7) for the smooth tube.

4.3. Correlation development

The present correlation for the smooth tube was modified from Bellinghausen and Renz's correlation [16] to simplify the calculations for practical applications. In spite of the correlation's poor agreement with their data [16], it is suggested for the Nusselt-type analysis including laminar film with stagnant vapour and a wave-free interface. For this reason, the low mass flux data ($29\ \mathrm{kg\ m^{-2}\ s^{-1}}$) were used. Fig. 14 compares the results from the present correlation with the experimental data. The majority of the data fall within ±20% of the proposed correlation. The correlation is expressed as follows:

$$\text{For the smooth tube}: \quad \delta^* = 7.4 Re_l^{0.018} \tag{4.7}$$

$$l = (k_l/L)\cdot(1/\delta^*) \tag{4.8}$$

$$\text{Liquid Reynolds number}: \quad Re_l = \dot{m}_r/(\pi \cdot D \cdot \mu_l) \tag{4.9}$$

$$\text{Liquid Nusselt number}: \quad Nu_l = 1/\delta^* \tag{4.10}$$

$$\text{Dimensionless film thickness}: \quad \delta^* = \delta/L \tag{4.11}$$

$$\text{Characteristic length}: \quad L = (\nu_l^2/g)^{1/3} \tag{4.12}$$

$$\text{Nusselt number}: \quad Nu_l = h_l \cdot L/k_l \tag{4.13}$$

5. Conclusion

The convective heat transfer coefficient of R134a was investigated during condensation in vertical downward flow at low and high mass fluxes in a smooth tube. To the best of the authors knowledge, research on the various parameters used in the present study is still limited. The results from this study are expected to fill the gap in the literature. The accurate and repeatable heat transfer data for the condensation of R134a in a downward flow at low and high mass flux inside a smooth tube were obtained. The effects of various relevant parameters such as condensing temperature, condensation temperature difference, vapour quality and mass flux on the heat transfer are discussed and investigated in detail.

A theoretical model from Carey [15] for downward condensation of R134a was used to investigate the local and average heat transfer coefficients in a vertical smooth tube at low mass flux conditions. The calculated results obtained from the modified Nusselt model incorporating the interfacial shear stress, along with the modified Nusselt model with McAdams correction factor and the

classical Nusselt model, were compared with the experimental data.

The condensation rate reaches the highest value at the pipe entrance where the highest local heat transfer coefficients exist. The film thickness is highest at the end of the tube where the local heat transfer coefficients are lowest.

Comparisons with laminar flow at low mass flux data show that the modified Nusselt model without a correction factor predicts the data well. Experimental results show that the interfacial shear stress that was incorporated into the modified Nusselt model affects the condensation process of R134a in a vertical smooth tube. The classical Nusselt theory and the McAdams heat transfer coefficient, which includes the wave effect between the phases, overestimate the data.

Comparisons with laminar flow at high mass flux show that Carey's theory, the McAdams correlation, and the classical Nusselt theory are inappropriate for the data. It should be noted that the Dobson and Chato model, Fujii correlation and Cavallini et al.'s correlation are good alternatives.

A new correlation for the determination of condensation heat transfer coefficients is proposed for practical applications, and as a result of this study, it is possible to simply calculate the condensation heat transfer coefficient with an interfacial shear effect during downward laminar flow in a vertical smooth tube.

Acknowledgements

The present study was financially supported by Yildiz Technical University and King Mongkut's University of Technology Thonburi (KMUTT). The first author wishes to thank KMUTT for providing him with a Post-doctoral fellowship, while the third author wish to acknowledge the support provided by the Thailand Research Fund.

References

[1] W. Nusselt, Die Oberflachen Kondenastion des Wasserdamfes, Z. Vereines Dtsch. Ingenieure 60 (1916) 541–546. 569–575.
[2] W.M. Rohsenov, J.H. Weber, A.T. Ling, Effect of vapor velocity on laminar and turbulent film condensation, Trans. ASME 78 (1956) 1637–1643.
[3] A.E. Dukler, Fluid mechanics and heat transfer in vertical falling film system, Chem. Eng. Prog. Symp. Series 56 (1960) 1–10.
[4] V.G. Levich, Physicochemical Hydrodynamics, Prentice-Hall, Englewood Cliffs, NJ, 1962.
[5] F. Blangetti, R. Krebs, E. Schlunder, Condensation in vertical tubes – experimental results and modelling, Chem. Eng. Fundam. (1982) 20–63.
[6] O.P. Bergelin, P.K. Kegel, F.G. Carpenter, C. Gazley, Co-current gas–liquid flow. II. flow in vertical tubes, Meeting at Berkeley, CA, USA, ASME, Heat Transfer and Fluid Mechanic Institute, 19–28 June 1946.
[7] N.K. Maheshwari, R.K. Sinha, D. Saha, M. Aritomi, Investigation on condensation in presence of a noncondensible gas for a wide range of Reynolds number, Nucl. Eng. Des. 227 (2004) 219–238.
[8] R.B. Bird, W.E. Steward, E.N. Lightfoot, Transport Phenomena, Wiley and Sons, Inc., New York, 1960. Chapter 21, pp. 642–666.
[9] R.G. Krebs, E.U. Schlünder, Condensation with non-condensing gases inside vertical tubes with turbulent gas and film flow, Chem. Eng. Prog. 18 (1984) 341–356.
[10] S.Z. Kuhn, V.E. Schrock, P.F. Peterson, An investigation of condensation from steam–gas mixtures flowing downward inside a vertical tube, Nucl. Eng. Des. 177 (1992) 53–69.
[11] P.F. Peterson, V.E. Schrock, S.Z. Kuhn, Recent experiments for laminar and turbulent film heat transfer in vertical tubes, Nucl. Eng. Des. 10 (1997) 157–166.
[12] S. Oh, A. Revankar, Analysis of the complete condensation in a vertical tube passive condenser, Int. Commun. Heat Mass Transfer 32 (2005) 716–727.
[13] W.H. McAdams, Heat Transmission, third ed., McGraw-Hill/University of California, New York/Berkeley, 1954. pp. 443.
[14] W.M. Kays, M.E. Crawford, Convective Heat and Mass Transfer, third ed., McGraw-Hill, New York, 1993.
[15] V.P. Carey, Liquid–Vapor Phase Change Phenomena, Hemisphere Publishing, 1992.
[16] R. Bellinghausen, U. Renz, Heat transfer and film thickness during condensation of steam flowing at high velocity in a vertical pipe, Int. J. Heat Mass Transfer 35 (1992) 683–689.
[17] S.J. Kline, F.A. McClintock, Describing uncertainities in single sample experiments, Mech. Eng. (1953). pp. 3.
[18] A.S. Dalkilic, Düşey borularda yoğuşmada ısı taşınım katsayısının araştırılması, Ph.D. Thesis, Yildiz Technical University, İstanbul, Turkey, 2007.
[19] M.O. McLinden, S.A. Klein, E.W. Lemmon, REFPROP, Thermodynamic and transport properties of refrigerants and refrigerant mixtures, NIST Standard Reference Database-version 6.01, 1998.
[20] M.K. Dobson, J.C. Chato, Condensation in smooth horizontal tubes, J. Heat Transfer Trans. ASME (1998) 193–213.
[21] O.G. Walladares, Review of in-tube condensation heat transfer correlations for smooth and microfin tubes, Heat Transfer Eng. 24 (2003) 6–24.
[22] A. Cavallini, J.R. Smith, R. Zecchin, A dimensionless correlation for heat transfer in forced convection condensation, in: Sixth International Heat Transfer Conference, Tokyo, Japan, pp. 309–313, 1974.
[23] G.F. Hewitt, D.N. Robertson, Studies of two-phase flow patterns by simultaneous X-ray and flash photography, Rept AERE-M2159, UKAEA, Harwell, 1969.
[24] S.L. Chen, F.M. Gerner, C.L. Tien, General film condensation correlations, Exp. Heat Transfer 1 (1987) 93–107.